

A Simplified Analytical Solution for the Computation of Machine Path in Filament Winding of Cylindrical Angle-Ply and Double-Double Structures

A. Andrianov^{1,*} and A.P.F. Militão²

University of Brasilia, Brazil

Abstract: This paper presents a simplified computation approach for the machine path (or winding trajectory) of grid structures and tubes with a circular cross-section and angle-ply or double-double layup. The solution for the machine path is given through controllable degrees of freedom of a low-cost two-axis filament winding machine (FWM): mandrel rotation and translation of the delivery eye along the axis of the mandrel. The efficiency of the analytical solution for the machine path of the FWM was ascertained by automated laying the cotton thread over the geodesic and non-geodesic groove imprinted on the surface of a cylindrical polylactide mandrel. These results validated the possibility of manufacturing cylindrical composite structures with an angle-ply layup or double-double stacking sequence, without the need for expensive software, making the winding technology accessible to society and promoting university extension.

Keywords: Filament winding, machine path, angle-ply, double-double, grid structure, composite tubes.

1. INTRODUCTION

Filament winding is a highly productive manufacturing method for polymer composite structures with a circular cross-section such as pipes and tubes [1] or grid and grid-stiffened cylindrical structures [2-4]. Over the past decade, several publications have addressed a variety of low-cost design solutions for filament winding machines (FWM) [5-10]. Such solutions are inspired by homemade computer numeric control (CNC) machines. Their structure and control system are based on slotted aluminum extrusions, OpenBuilds and 3D printed parts, off-the-shelf electronic components and open-source software [11]. However, there are no low-cost solutions for the generation of a machine path given by the coordinates of the delivery eye in relation to the surface of the mandrel.

Several commercial programs are available in today's market for generating filament winding trajectories [12]. Their price corresponds to the cost of the FWM. Thus, the programs are not financially affordable for evolving small companies and start-ups, whose activities relate to the design and manufacturing of cylindrical composite structures.

The alternative solution to make winding technology more cost-effective is the development of analytical solutions to determine the machine path [13]. Based on the analytic geometry, the kinematic equations for the machine path were derived for square tubes [14], pressure vessels [15-16] and T-shaped structures [17]. Several analytical solutions provided in the scientific literature for the calculation of winding trajectories [13, 18] require a profound knowledge of programming or

mathematics from an FWM operator. Recently, analytical equations to compute the coordinates of the delivery eye trajectory for the cylindrical structure were provided in reference [15]. The equations were adapted from a mathematical model for an involute screw surface analytically described in a Cartesian coordinate system [19]. However, the solution considered neither the reverse direction of the winding nor the non-geodesic fiber pathways.

Thus, the main objective of this work is to obtain simple and comprehensive analytical equations for the machine path in filament winding of angle-ply and double-double grid structures or tubes with a circular cross-section. The mathematical approach adopted in the methodology for the derivation of executive expressions is based only on analytic geometry. The solution for the winding trajectory is given through three coordinates of the delivery eye in a Cartesian coordinate system in terms of the mandrel's geometry and the winding parameters for both geodesic and non-geodesic fiber pathways. The solution for the machine path is given through controllable degrees of freedom of a two-axis FWM: rotation of the mandrel and translation of the delivery eye along the mandrel's axis.

2. METHODOLOGY

2.1. Models

The model of a grid structure under consideration is formed by a series of spiral space curves that intersect on a cylindrical surface (Figure 1a). These curves represent both geodesic and non-geodesic fiber pathways on the cylindrical surface of a mandrel. The curves are equidistantly distributed over the cylindrical surface in the direction of a generating line, so the angle Φ_g between two adjacent spiral curves of the

*Address correspondence to this author at the University of Brasilia, Brazil; E-mail: andrianov@aerospace.unb.br

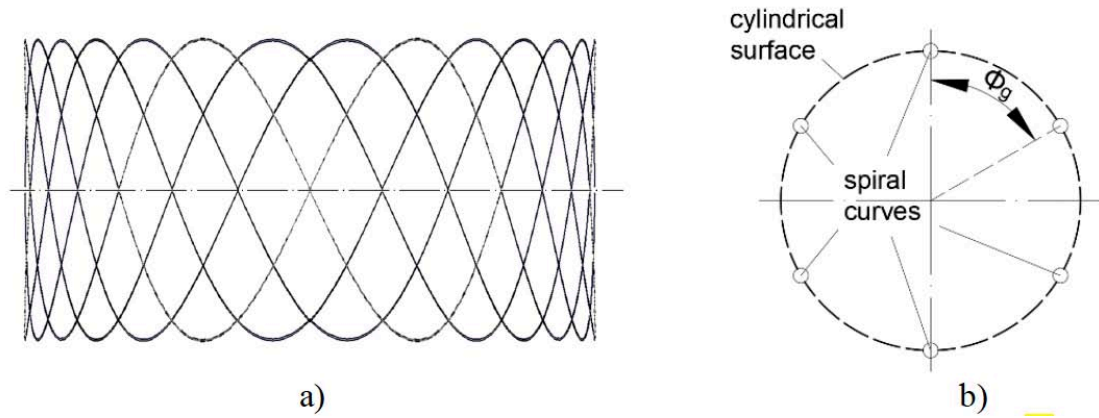


Figure 1: The model of a grid structure with **a)** a series of 6 cycles of a fiber/tow and **b)** its cross-section.

grid structure measured in the direction of the mandrel rotation (Figure 1b). This structure can be manufactured by filament winding, where a fiber (or a tow) is laid along the spiral path of the curve on the surface of the cylindrical mandrel. The fiber crosses twice any latitude of the mandrel in a winding cycle. Here, it is assumed that the winding cycle corresponds to the fiber path from a reference latitude at one end of the mandrel to its other end with a return to the reference latitude. Thus, a stroke is the laying of the fiber in one of the directions along the mandrel's axis (forward or return one) and corresponds to half of a winding cycle (Figure 2). The fiber crosses any latitude of a mandrel only once in a forward or return stroke.

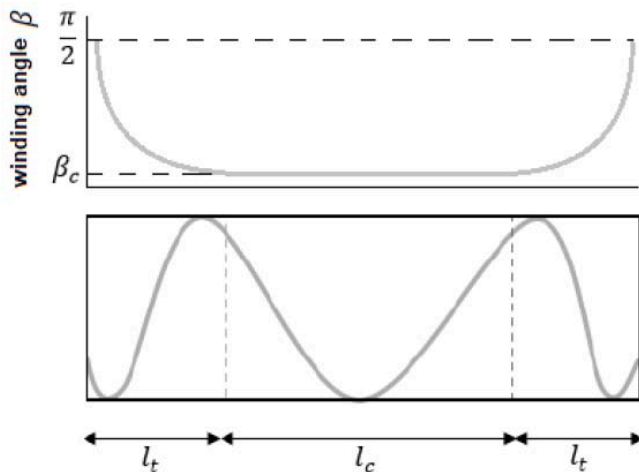


Figure 2: Fiber path (helical curve) on the surface of the cylindrical mandrel for one stroke.

A stroke can be given through two types of fiber pathways on the surface of the cylindric mandrel (Figure 2): 1) the geodesic path with a constant winding angle β_c ($0 < \beta_c < \pi/2$), which corresponds to the regular part of the structure l_c , and 2) the non-geodesic path, where the winding angle varies along the mandrel's length l_t from 90 degrees to β_c and vice versa. This length l_t corresponds to the transient part of the structure. The model of a tube (or a pipe) is similar to the above-mentioned model of a grid

structure except for the fact that the tow with a pre-defined width covers the entire cylindrical surface forming an angle-ply cylindrical laminate.

2.2. Winding Parameters

For both models, l_c is the required length of the structure, while for the model of a tube, the transition length l_t is a function of the friction coefficient μ between the fiber and the mandrel's surface, the radius of the cylinder R_c and the winding angle β_c [20]:

$$l_t = \frac{R_c}{2\mu} \left[\left(\tan^{-1} \frac{\beta_c}{2} + \tan \frac{\beta_c}{2} \right) - \left(\tan^{-1} \frac{\pi}{2} + \tan \frac{\pi}{2} \right) \right] \quad (1)$$

Considering that the axisymmetric structures can be wound utilizing the FWM with two controllable axes [13], the fiber path can be given through the angle of mandrel rotation or turn-around angle Φ , which is a function of the z-coordinate (along the axis of revolution of the mandrel). The winding parameter Φ is defined following the methodology and recommendations detailed in [15].

The turn-around angle for the regular part of the structure is given by the equation

$$\Phi_c(z) = \frac{z \cdot \tan(\beta_c)}{R_c} \quad (2)$$

The turn-around angle for the transient part of the structure is given by the equation:

$$\Phi_t(z) = \frac{1}{\mu} \cdot \ln \left[\frac{\frac{1 + \cos(\beta_c)}{\sin(\beta_c)}}{\frac{1}{\sin(\beta_c)} - z \cdot \frac{\mu}{R_c} + \sqrt{\left(\frac{1}{\sin(\beta_c)} - z \cdot \frac{\mu}{R_c} \right)^2 - 1}} \right] \quad (3)$$

The integration of equation (3) from 0 to l_t gives a total turn-around angle for the transient part:

$$\Phi_t = \frac{1}{\mu} \cdot \ln \left(\frac{\sin(\beta_c)}{1 - \cos(\beta_c)} \right) \quad (4)$$

The turn-around angle for one winding cycle is given as follows

$$\Phi_1 = 2\Phi_c + 4\Phi_t \quad (5)$$

The tow after one winding cycle returns to the same latitude from which it started its trajectory but does not necessarily coincide with the starting point. It happens when the obtained value Φ_1 is not a multiple of 360° . The angular pitch of winding Φ_p^* is defined as an angle measured in the direction of the mandrel rotation between the starting and final points of one winding cycle and can be described mathematically as:

$$\Phi_p^* = \Phi_1 - 2\pi \cdot \text{integer} \left(\frac{\Phi_1}{2\pi} \right) \quad (6)$$

The angular pitch Φ_p^* must be increased to the closest angle Φ_p , which is a multiple of 360° (60° , 72° etc.).

The difference between the accepted and calculated angular pitch, Φ_f , distributed uniformly between two flanges of the mandrel, can be given as:

$$\Phi_f = \frac{\Phi_p - \Phi_p^*}{2} \quad (7)$$

This angle hereinafter is referred to as a compensation angle. As larger is Φ_f as more excessive tow material is built up over the flanges.

To ensure full coverage of the mandrel with a composite material for the model of a tube, the cycle must be repeated a sufficient number of times with correctly chosen increments of mandrel rotation between cycles. The corresponding incremental turn-around angle Φ_w depends on the tow's width b :

$$\Phi_w = \frac{b}{R_c \cdot \cos(\beta_c)} \quad (8)$$

The angle Φ_w hereinafter is referred to as an offset angle.

The angular pitch and the compensation angle are used to define a pattern of the wound tube and, together with the offset angle a configuration of the grid structure.

2.3. Validation of the Analytical Solution for the Machine Path

The efficiency of the solution for the machine path was verified by laying the cotton thread along the geodesic and non-geodesic paths marked on the surface of a cylindrical mandrel. The mandrel with continuous grooves along the paths is printed with polylactide filament. The coordinates of the geodesic and non-geodesic paths were calculated by equations from the previous subsection. The G-code for controlling the two axes of the FWM was compiled manually after the discretization of the derived analytical solutions.

3. RESULTS AND DISCUSSIONS

3.1. Analytical Solution

Figure 3a shows a cylindrical mandrel with a Cartesian coordinate system, whose origin is in the center of the base. Winding is carried out under conditions when the minimum distance R_E between delivery eye E and spindle axis z is constant. The curve AM is the fiber laid on the cylindrical surface of the mandrel. The line ME shows the fiber length (denominated as λ) between the delivery eye E and point M where the fiber is tangent to the surface of the mandrel. The coordinates of the fiber path on the surface of the mandrel are functions of the winding angle β and the turn-around angle Φ :

$$x = R_c \cos(\Phi), y = R_c \sin(\Phi), z = R_c \frac{\Phi}{\tan(\beta)} \quad (9)$$

The winding angle in the transition part of the mandrel depends on the z -coordinate and can be found by modifying the third from equations (9) as following

$$\beta_t(z) = \text{atan} \left(R_c \frac{d\Phi_t(z)}{dz} \right) \quad (10)$$

Derivative of (3) with respect to z is given as

$$\frac{d\Phi_t(z)}{dz} = \frac{1}{\mu} \cdot \left[\frac{\frac{\mu}{R_c} \left(1 + \frac{F(z)}{\sqrt{F(z)^2 - 1}} \right)}{F(z) + \sqrt{F(z)^2 - 1}} \right], \quad (11)$$

where

$$F(z) = \frac{1}{\sin(\beta_c)} - z \cdot \frac{\mu}{R_c} \quad (12)$$

Equation (3) may yield a complex number for some initial conditions. If this occurs, only the real part must be considered.

The length λ is constant for the regular part and can be computed from Figure 3a as following

$$\lambda_c = \frac{MK}{\sin \beta_c}, \quad (13)$$

where MK can be determined from Figure 3b as

$$MK = \sqrt{R_E^2 - R_c^2}, \quad (14)$$

The length λ is variable along the z -axis for the transient part of the mandrel since it depends on the winding angle $\beta_t(z)$ as follows

$$\lambda_t(z) = \frac{MK}{\sin \beta_t(z)}. \quad (15)$$

The x and y coordinates of the delivery eye are given as

$$x_{EI} = OG \cos(\alpha + \Phi), y_{EI} = OG \sin(\alpha + \Phi). \quad (16)$$

Considering that $OG = R_E$ and we may rewrite equations (16) as follows

$$\begin{aligned}x_{EI} &= R_E[\cos(\alpha) \cos(\Phi) - \sin(\alpha) \sin(\Phi)], \\y_{EI} &= R_E[\cos(\alpha) \sin(\Phi) + \sin(\alpha) \cos(\Phi)].\end{aligned}\quad (17)$$

From the right trapezoid BMEG (Figure 3a), we have

$$BG = \lambda \sin(\beta), \quad z_{EI} = EK + KG, \quad (18)$$

where

$$EK = \lambda \cos(\beta), \quad KG = z \quad (19)$$

From the triangle BOG, we have

$$\cos(\alpha) = \frac{R_c}{R_E}, \quad \sin(\alpha) = \frac{BG}{R_E}. \quad (20)$$

Substitution of equations (19) into the second from equations (18) and equations (20) into equations (17) yields the coordinates of the machine path for the forward stroke (Figure 3a)

$$\begin{aligned}x_{EI} &= R_c \cos(\Phi) - \lambda \sin(\Phi) \sin(\beta), \\y_{EI} &= R_c \sin(\Phi) + \lambda \sin(\Phi) \cos(\beta), \\z_{EI} &= z + \lambda \cos(\beta)\end{aligned}\quad (21)$$

For the return stroke, the coordinate y changes its sign and the coordinate z is determined from Figure 3c.

$$\begin{aligned}x_{EV} &= R_c \cos(\Phi) - \lambda \sin(\beta) \sin(\Phi), \\y_{EV} &= -[R_c \sin(\Phi) + \lambda \sin(\beta) \cos(\Phi)], \\z_{EV} &= z - \lambda \cos(\beta)\end{aligned}\quad (22)$$

The winding parameters in equations (21) and (22) are determined in accordance with Table 1 depending on the part of the structure to be wound: regular or transient.

The following condition can be used to check whether the values of the x and y coordinates are correct:

$$R_E = \sqrt{x_{EI}^2 + y_{EI}^2} = \sqrt{x_{EV}^2 + y_{EV}^2} = const. \quad (23)$$

The machine path in terms of controllable degrees of freedom of the two-axis FWM is given as follows:

$$X = \frac{180}{\pi} \Phi_x(z), \quad Y = z_E = z \pm \lambda \cos(\beta) \quad (24)$$

where subscript x is substituted by t or c depending on the part to be wound, X is the angle of rotation of the mandrel (in degrees) and Y is the linear translation of the delivery eye along the mandrel's axis.

3.2. Examples of the Machine Path Computation

The initial data for the filament winding of an 80 mm diameter tube are given in Table 2. The layup [45°/-45°] is typical for those structures that work in conditions of pure torsion. The value of accepted μ corresponds to the friction coefficients that are common for dry winding (with the pre-impregnated roving) [21]. The length of the tube has been chosen in such a way that the mandrel would make a complete revolution ($\Phi_c = 360^\circ$) after one stroke (Table 3). According to the data given in Tables 2 and 3, the minimum length for the cylindrical mandrel must be equal to 416.7 mm.

To decrease the computational volume, the origin of a Cartesian coordinate system was placed on the axis

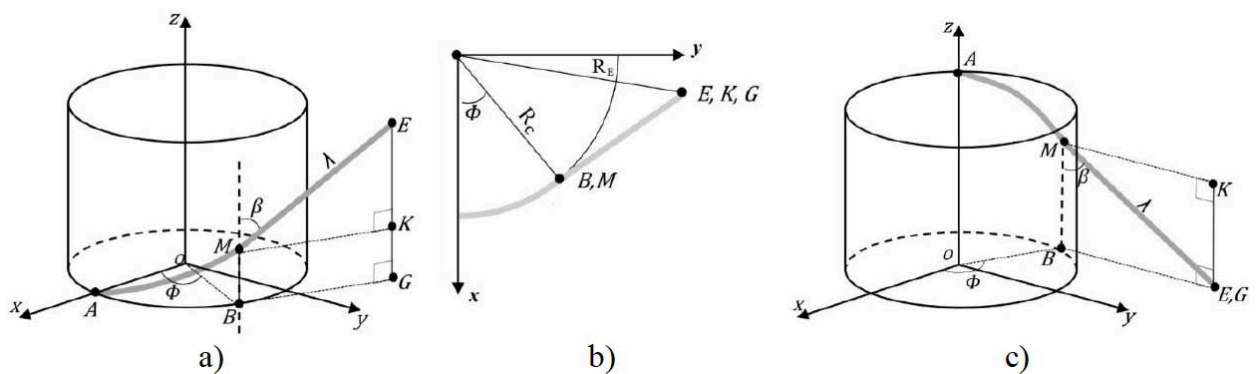


Figure 3: Model of a filament winding on cylindrical mandrel: **a)** the forward stroke, **b)** projection of the fiber on the xy-plane for the forward stroke, **c)** the return stroke.

Table 1: The Winding Parameters for the Coordinates of the Machine Path

Part of the mandrel	Turn-around angle Φ	Winding angle β	Fiber length λ
regular	$\Phi_c(z)$	$\beta_c = const$	$\lambda_c = const$
transient	$\Phi_t(z)$	$\beta_t(z)$	$\lambda_t(z)$

Table 2: Design Characteristics of the Tube Ø80 mm

R_c , mm	l_c , mm	β_c , °	b , mm	μ
40	251	±45	3.5	0.2

Table 3: Winding Parameters for the Tube Ø80 mm

l_t , mm	$\Phi_c(l_c)$, °	Φ_t , °	Φ_1 , °	Φ_p^* , °	Φ_p , °	Φ_f , °	Φ_w , °
82.843	359.531	252.495	1792.042	289.042	300.000	5.479	7.090

of symmetry of the mandrel in the interface plane between the regular and transient parts in such a way that the z-axis would be along the axis of revolution. Figure 4a shows half of the mandrel and the fiber path from the center of the regular part to the end of the transient part with the corresponding trajectory for the delivery eye. The minimum distance $R_E = 58.31 \text{ mm}$ was chosen in such a way that the fiber length λ would be equal to 60 mm. The coordinates of the fiber path for the regular part are given by the first two equations (9), where the angle Φ is replaced by the $\Phi_c(z)$ from equation (2) and the z-coordinate varies in the interval

$$-l_c/2 \leq z \leq 0 \quad (25)$$

Equations (9) yield the coordinates for the transient part. Here, Φ is replaced by the $\Phi_t(z)$ from equation (3) and the z-coordinate varies in the interval

$$0 \leq z \leq l_t \quad (26)$$

The machine path for the forward stroke is computed by equations (21) with the use of data from Table 1.

The fiber path of the return stroke shown in Figure 4b must be coordinated with the fiber path of the forward stroke taking into consideration the position of the origin of the coordinate system and the intervals (25) and (26). The coordinates of the fiber path for the

return stroke are determined by the same equations as for the forward stroke, however, the y-coordinate changes its sign, and the turn-around angle $\Phi_x(z)$ must be corrected. The corrected turn-around angles $\bar{\Phi}_x(z)$ for the regular and transient parts are defined respectively as

$$\bar{\Phi}_c(z) = \Phi_c(z) + \varphi_f, \bar{\Phi}_t(z) = \Phi_t(z) + \varphi_f, \quad (27)$$

where φ_f is the coordinating angle for the fiber path defined as

$$\varphi_f = 2\Phi_t. \quad (28)$$

The machine path for the reverse stroke is computed by equations (22) with the use of data from Table 1, where the turn-around angle $\Phi_x(z)$ must be corrected. The corrected turn-around angles $\bar{\Phi}_x(z)$ for the regular and transient parts are defined by equations (27), where φ_f is substituted by the coordinating angle for the machine path φ_e defined as

$$\varphi_e = 2 \left[\pi - \Phi_t - \text{atan} \left(\frac{\lambda \sin \beta_c}{R_c} \right) \right]. \quad (29)$$

The coordinates of the delivery eye are computed only for one cycle. To obtain a tube, the cycle must be repeated a sufficient number of times with correctly chosen increments of mandrel rotation Φ_w between cycles. It is important to note that the interval for z must be discretized for the transient part, while for the

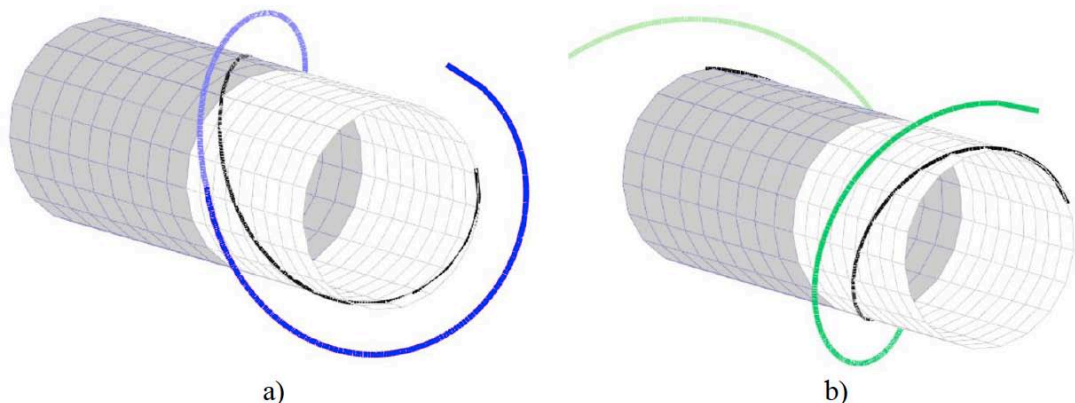


Figure 4: The fiber path and the trajectory of the delivery eye for half of the mandrel, whose dark and light surfaces correspond to the regular and transient part respectively: **a)** the forward stroke, **b)** the return stroke.

regular part it is sufficient to calculate only the coordinates of the beginning and the end of the trajectory. This can be explained by the fact that the winding angle is constant in the regular part, and the relationship between X and Y controllable DOFs is linear.

The results of the computation are presented in Table A1 of Appendix A for both forward and return strokes. The delivery eye trajectory related to the transient part was discretized into eleven intervals. It must be noted that the values for the return stroke are not in agreement with the physics of the winding process: the turn-around angle is decreasing while in filament winding the mandrel always rotates only in one direction independently of the stroke. Furthermore, the singularity in the function $\beta_t(z)$ is observed when $z = l_t$. Therefore, the coordinates z_E and ϕ for this point must be computed by equations (1) and (4) respectively (the values in square brackets in Table A1).

The initial position of the delivery eye E to begin the winding process is in front of one of the mandrel's ends as shown in Figure A1 of Appendix A. Shifting the origin of the coordinate system from the interface between the parts to the mandrel's end requires a reformulation of equations (28 – 29). To avoid this, the translational motion of the delivery eye can be given in terms of incremental positioning, that is, through the command G91 of the G-Code used in CNC programming. In this case, the coordinates computed by equations (21 – 22) must be given through the incremental coordinates:

$$\Phi_j^i = \Phi_{j+1} - \Phi_j, z_j^i = z_{E,j+1} - z_{E,j}, \quad (30)$$

where $\Phi_j, z_{E,j}$ and $\Phi_{j+1}/z_{E,j+1}$ are the coordinates of the initial and final position of the delivery eye for the given discretization interval i .

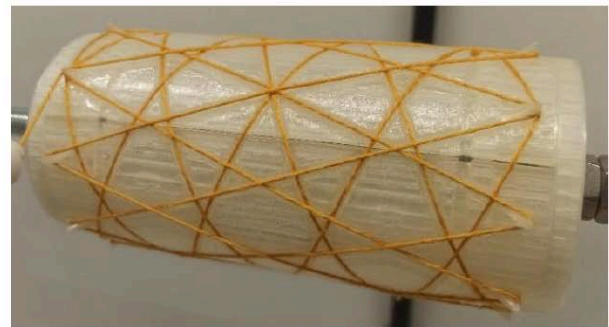
The incremental coordinates computed by equations (30) were used to compile the G-code for the filament winding of a Ø80 mm tube (Table A2 of Appendix A). It is worth noting that the G-code can be applied for the filament winding of a Ø80 mm grid structure with a series of N cycles after corrections in the number of cycles and both the compensation and the offset angles. In this case, the turn-around angles Φ_f and Φ_w additionally define the configuration of the grid structure and must be equal to 35.48° and 60° respectively for a series of 6 cycles. The mentioned corrections are enclosed in round parentheses reserved for comments in the G-code. The validation of the compiled G-code with the use of a two-axis FWM showed that the fibers were laid along the geodesic and non-geodesic paths marked on the surface of the printed cylindrical mandrel (Figure 5a).

It must be emphasized that for a grid structure, the friction coefficient μ defines the geometry of the fiber path in the transient part of the mandrel. For the filament winding of tubes or pipes, the minimum friction coefficient depends on the materials of the tow and mandrel in contact. Low friction coefficients common for wet filament winding [21] lead to an exaggerated length of the transient part.

The grid structure with a double-double configuration shown in Figure 5b does not have a transitional part. The non-slippage condition at the flanges of the mandrel is realized through the pins



a)



b)

Figure 5: Examples of the wound structures: **a)** the grid structure with a 6-cycle angle-ply layup [$\pm 45^\circ$], **b)** the grid structure with a double-double configuration [$\pm 20^\circ/\pm 65.4^\circ$].

Table 4.: Characteristics of the Wound Grid Structure with a Double-Double Configuration

Geometry				Winding parameters					
$\beta_c, ^\circ$	R_c, mm	l_c, mm	N_c	λ, mm	R_E, mm	$\Phi_c(l_c), ^\circ$	$\Phi_p, ^\circ$	$\Phi_f, ^\circ$	$\Phi_w, ^\circ$
20.0	40	153.4	9	100.0	52.6	80.00	180.00	0.00	0.00
65.4	40	153.4	3	37.6	52.6	480.00	270.00	0.00	0.00

printed together with the mandrel. The geometry and winding parameters of the grid structure are given in Table 4, where N_c is the number of cycles.

CONCLUSIONS

The presented paper validates the possibility of manufacturing simple axisymmetric structures, such as tubes and cylindrical grid structures, through filament winding without the use of sophisticated equipment and commercial software. Equations for controlling a filament winding machine with two controllable axes are obtained by referring to analytical geometry only and do not require additional efforts or specific skills from the FWM operator. Formally, the solution can be presented in the form of a simple electronic office document such as a spreadsheet.

Preliminary results of winding tubes and grid structures with circular sections showed that the delivery eye lays the fiber on the predetermined geodesic and non-geodesic path for composite structures with an angle-ply layer $[\pm\beta]$. The suggested solution allows competition teams or technological research and development groups, startups and small companies to carry out their projects, thus making filament winding technology more accessible to society and promoting university extension.

DECLARATION OF COMPETING INTEREST

The authors declare no conflict of interest.

FUNDINGS

This work was supported by the Foundation of Research Projects in the Federal District, grant number FAP DF 00193-00000809/2021-18.

APPENDIX

Table A1: Coordinates of the Machine Path for One Cycle Computed by Equations (21) and (22)

Stroke	Part	z, mm	X, deg	Y, mm	Stroke	Part	z, mm	X, deg	Y, mm
forward	regular	-251.00	-359.53	-208.57	reverse	transient	*82.84	[252.50]	[82.84]
		0	0	42.43			74.56	170.32	62.22
	transient	0	0	42.43			66.27	136.67	48.65
		8.28	12.23	48.19			57.99	111.11	36.19
		16.57	25.28	53.86			49.71	89.78	24.29
		24.85	39.29	59.42			41.42	71.16	12.74
		33.14	54.49	64.85			33.14	54.49	1.42
		41.421	71.16	70.11			24.85	39.29	-9.72
		49.71	89.78	75.12			16.57	25.28	-20.72
		57.99	111.11	79.79			8.28	12.23	-31.62
		66.27	136.67	83.9			0	0	-42.43
		74.56	170.32	86.9			0	-238.36	-42.43
		*82.84	[252.50]	[82.84]			-251.00	-597.89	-293.43

*To provide a continuous winding at the end of the mandrel, it is recommended to evaluate X by equation (4) for the last interval $z = l_t$ while Y must be equal to l_t . The latter condition assumes that the initial position of the delivery eye E to begin a new stroke must be in front of the mandrel's end.

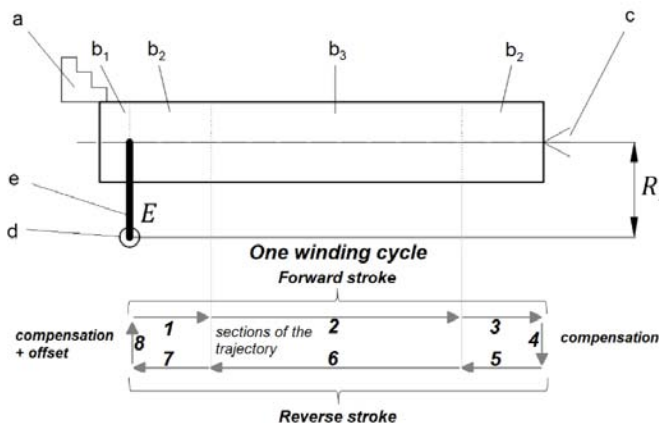


Figure A1: The initial position of the delivery eye in a winding cycle: a – lathe chuck, b – mandrel (b_1 – clamped part, b_2 – transient part, b_3 – regular part), c – tailstock, d – delivery eye, e – fiber/tow.

Table A2: An example of the G-code for the filament winding on the mandrel with imprinted geodesic and non-geodesic paths (installation in accordance with Figure A1 where $R_E = 58.31$ mm).

Program	
O0101 (G-code for a Ø80 mm tube or a Ø80 mm grid structure with a series of 6 cycles) F7000 (winding speed: rotation of the mandrel X in degrees per minute) M98 P010 L1 (call for subprogram 010: # of angle-plyes) M30 (program end)	
Subprograms	
O010 (angle-plyes) M98 P001 L9 (call for subprogram 001: # of series, L6 for the grid structure) M99 (subprogram end)	O001 (series) M98 P002 L5 (call for subprogram 002: # of cycles with Φ_f , L0 for the grid structure) M98 P007 L1 (call for subprogram 007: # of cycles with both Φ_f and Φ_w) M99 (subprogram end)
O002 (one cycle with Φ_f) M98 P003 L1 (call for subprogram 003: # of forward strokes) M98 P005 L1 (call for subprogram 005: Φ_f) M98 P004 L1 (call for subprogram 004: # of reverse strokes) M98 P005 L1 (call for subprogram 005: Φ_f) M99 (subprogram end)	O007 (one cycle with both Φ_f and Φ_w) M98 P003 L1 (call for subprogram 003: # of forward strokes) M98 P005 L1 (call for subprogram 005: Φ_f) M98 P004 L1 (call for subprogram 004: # of reverse strokes) M98 P006 L1 (call for subprogram 006: $\Phi_f + \Phi_w$) M99 (subprogram end)
O003 (forward stroke) (transition part, section 1 of a cycle) G91 X 82.175 Y 20.62 G91 X 33.65 Y 13.57 G91 X 25.56 Y 12.46 G91 X 21.33 Y 11.9 G91 X 18.62 Y 11.55 G91 X 16.67 Y 11.32 G91 X 15.2 Y 11.14 G91 X 14.01 Y 11 G91 X 13.05 Y 10.9 G91 X 12.23 Y 10.81 (regular part, section 2 of a cycle) G91 X 359.530 Y 251 (transition part, section 3 of a cycle) G91 X 12.23 Y 5.76 G91 X 13.05 Y 5.67 G91 X 14.01 Y 5.56 G91 X 15.2 Y 5.43 G91 X 16.67 Y 5.26 G91 X 18.62 Y 5.01 G91 X 21.33 Y 4.67 G91 X 25.56 Y 4.11 G91 X 33.65 Y 3 G91 X 82.175 Y -4.06 M99 (subprogram end)	O004 (reverse stroke) (transition part, section 5 of a cycle) G91 X 82.175 Y -20.62 G91 X 33.65 Y -13.57 G91 X 25.56 Y -12.46 G91 X 21.33 Y -11.9 G91 X 18.62 Y -11.55 G91 X 16.67 Y -11.32 G91 X 15.2 Y -11.14 G91 X 14.01 Y -11 G91 X 13.05 Y -10.9 G91 X 12.23 Y -10.81 (regular part, section 6 of a cycle) G91 X 359.530 Y -251 (transition part, section 7 of a cycle) G91 X 12.23 Y -5.76 G91 X 13.05 Y -5.67 G91 X 14.01 Y -5.56 G91 X 15.2 Y -5.43 G91 X 16.67 Y -5.26 G91 X 18.62 Y -5.01 G91 X 21.33 Y -4.67 G91 X 25.56 Y -4.11 G91 X 33.65 Y -3 G91 X 82.175 Y 4.06 M99 (subprogram end)
O005 (Φ_f; section 4 of a cycle) G91 X 5.48 Y 0 (X 35.48 for the grid structure) M99 (subprogram end)	O006 ($\Phi_f + \Phi_w$; section 8 of a cycle) G91 X 5.48 Y 0 (X 35.48 for the grid structure) G91 X 7.09 Y 0 (X 60 for the grid structure) M99 (subprogram end)

ACKNOWLEDGEMENTS

The authors sincerely acknowledge the Foundation of Research Projects in the Federal District (FAP DF) for the financial support for the project.

CREDIT AUTHOR STATEMENT

Andrianov A: Conceptualisation; Methodology; Resources; Supervision; Writing – original draft; Writing

– review. Militão APF: Data curation; Formal Analysis; Writing – original draft.

REFERENCES

- [1] Green JE, Automated Filament Winding Systems. In: Peters ST, editor. Composite Filament Winding. ASM International: Materials Park 2011; pp. 7-18
- [2] Huybrechts S, Hahn S, Meink T. Grid Stiffened Structures: A Survey of Fabrication, Analysis and Design Methods. In:

- International Conference on Composite Materials. Paris, 1999. Available from: <https://www.iccm-central.org/Proceedings/ICCM12proceedings/site/papers/pap357.pdf>
- [3] Vasiliev VV, Barynin VA, Rasin AF. Anisogrid lattice structures – survey of development and application. *Composite Structures* 2001; 54: 361-370. [https://doi.org/10.1016/S0263-8223\(01\)00111-8](https://doi.org/10.1016/S0263-8223(01)00111-8)
- [4] Vasiliev VV, Barynin VA, Razin AF. Anisogrid composite lattice structures – Development and aerospace applications. *Composite Structures* 2012; 94: 1117-1127. <https://doi.org/10.1016/j.compstruct.2011.10.023>
- [5] Abdalla FH, Mutasher SA, Khalid YA, Sapuan SM, Hamouda AMS, Sahari BB, Hamdan MM. Design and Fabrication of Low Cost Filament Winding Machine. *Mater Des* 2007; 28: 234-239. <https://doi.org/10.1016/j.matdes.2005.06.015>
- [6] Mateen MA, Shankar DVR, Hussain MM. Design and Development of Low Cost Two Axis Filament Winding Machine. *J Adv Manuf Technol* 2018; 12: 117-126. Available from: <https://jamt.utm.edu.my/jamt/article/view/1862/3349>
- [7] Krishnamurthy TN, Idkan M. Fabrication of Low Cost Filament Winding Machine. *Int J Recent Trends Electr Electron Eng* 2014; 4: 30-39.
- [8] Mutasher S, Mir-Nasiri N, Lin LC. Small-Scale Filament Winding Machine for Producing Fiber Composite Products. *J Eng Sci Technol* 2012; 7: 156-168.
- [9] Quanjin M, Rejab MRM, Sahat IM, Amiruddin M, Bachtiar D, Siregar JP, Ibrahim MI. Design of Portable 3-Axis Filament Winding Machine with Inexpensive Control System. *J Mech Eng Sci* 2018; 12: 3479-3493. <https://doi.org/10.15282/jmes.12.1.2018.15.0309>
- [10] Quanjin M, Rejab MRM, Kumar NM, Idris MS. Experimental Assessment of the 3-Axis Filament Winding Machine Performance. *Results Eng* 2019; 2: 100017. <https://doi.org/10.1016/j.rineng.2019.100017>
- [11] Hunt CJ, Wisnom MR, Woods BKS. WrapToR Composite Truss Structures: Improved Process and Structural Efficiency. *Compos Struct* 2019; 230: 111467. <https://doi.org/10.1016/j.compstruct.2019.111467>
- [12] Sofi T, Neunkirchen S, Schledjewski R. Path Calculation, Technology and Opportunities in Dry Fiber Winding: A Review *Adv Manuf Polym Compos Sci* 2018; 4: 57-72. <https://doi.org/10.1080/20550340.2018.1500099>
- [13] Mazumdar SK, Hoa SV. Analytical Models for Low Cost Manufacturing of Composite Components by Filament Winding, Part I: Direct Kinematics. *Journal of Composite Materials* 1995; 29 (11): 1515-1541. <https://doi.org/10.1177/002199839502901106>
- [14] Zu L, Xu H, Zhang B, Li D, Zi B, Zhang B. Design and production of filament-wound composite square tubes. *Composite Structures* 2018; 191: 202-208. <https://doi.org/10.1016/j.compstruct.2018.02.069>
- [15] Andrianov A, Tomita EK, Veras CAG, Telles BA. Low-Cost Filament Winding Technology for University Laboratories and Startups. *Polymers* 2022; 14: 1066. <https://doi.org/10.3390/polym14051066>
- [16] Abdel-Hady F. Filament Winding of Revolution Structures. *J Reinf Plast Compos* 2005; 24: 855-868. <https://doi.org/10.1177/0731684405047772>
- [17] Seereerem S, Wen JTY. An all-Geodesic algorithm for filament winding of a T-shaped form. *IEEE Trans Ind Electron* 1991; 38: 484-90. <https://doi.org/10.1109/41.107105>
- [18] Koussios S, Bergsma OK, Beukers A. Filament Winding. Part 2: Generic Kinematic Model and Its Solutions. *Compos Part A Appl Sci Manuf* 2004; 35: 197-212. <https://doi.org/10.1016/j.compositesa.2003.10.004>
- [19] Radzevich SP. *Geometry of Surfaces*. 2nd ed. Springer Nature: Cham, Switzerland; 2020.
- [20] Scholliers J. Robotic filament winding of asymmetric composite parts; 1994. Available from: <https://lirias.kuleuven.be/retrieve/224495>
- [21] Reynolds H. Pressure vessel design, fabrication, analysis, and testing. In: Peters ST, editor. *Composite Filament Winding*. ASM International: Materials Park 2011; pp. 115-148.

Received on 06-11-2022

Accepted on 05-12-2022

Published on 16-12-2022

<https://doi.org/10.6000/1929-5995.2022.11.07>

© 2022 Andrianov and Militão; Licensee Lifescience Global.

This is an open access article licensed under the terms of the Creative Commons Attribution License (<http://creativecommons.org/licenses/by/4.0/>) which permits unrestricted use, distribution and reproduction in any medium, provided the work is properly cited.